ULTRASOUND NEWS

September, 2025

Chinese Taipei Society of Ultrasound in Medicine

Available online at www.sciencedirect.com

ScienceDirect

journal homepage: www.jmu-online.com

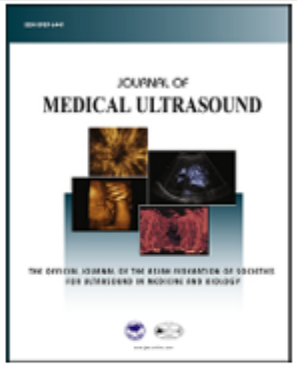

ORIGINAL ARTICLE

A Standardized Ultrasound Scoring System for Preoperative Prediction of Difficult Laparoscopic Cholecystectomy☆

Mohammed Azfar Siddiqui [1*], Syed Amjad A. Rizvi [2], Sara Sartaj [3], Ibne Ahmad [4], Syed Wajahat A. Rizvi [3]

[1] *Department of Radiology, Saint Louis University, MO, USA,* [2] *Department of Surgery, Jawaharlal Nehru Medical College, Aligarh, India,* [3] *Jawaharlal Nehru Medical College, Aligarh, India, and* [4] *Department of Radiodiagnosis, Jawaharlal Nehru Medical College, Aligarh, India*

Abstract *Purpose:* Laparoscopic cholecystectomy (LC) has become the treatment of choice for cholelithiasis. Still some patients required conversion to open cholecystectomy (OC). Our aim was to develop a standardized Ultrasound based scoring system for preoperative prediction of difficult LC.
Methods and materials: Ultrasound findings of 300 patients who underwent LC were reviewed retrospectively. Four parameters (time taken, biliary leakage, duct or arterial injury, and conversion) were analyzed to classify LC as easy or difficult. The following ultrasound findings were analyzed: GB wall thickness, pericholecystic collection, distended GB, impacted stones, multiple stones, CBD diameter and liver size. Out of seven parameters, four were statistically significant in our study. A score of 2 was assigned for the presence of each significant finding and a score of 1 was assigned for the remaining parameters to a total score of 11. A cut-off value of 5 was taken to predict easy and difficult LC.
Results: 66 out of 83 cases of difficult LC and 199 out of 217 cases of easy LC were correctly predicted on the basis of scoring system. A score of >5 had sensitivity 80.7% and specificity 91.7% for correctly identifying difficult LC. Prediction came true in 78.8% difficult and 92.6% easy cases. US findings of GB wall thickness, distended GB, impacted stones and dilated CBD were found statistically significant.

Statistical methods

All statistical analyses were performed with the SPSS 15.0 for Windows (SPSS Inc, Chicago, IL) and Microsoft word have been used to generate tables. The two-tailed chi-square test has been used to find the significant association of findings of preoperative ultrasonographic score with per-operative outcome of difficult LC. A p value <0.05 was considered to be significant. The sensitivity, specificity along with positive predictive values for predicting easy and difficult cases were calculated.

Results

There were 316 cases that underwent LC for symptomatic GB disease. 16 patients who underwent conversion because of equipment failure, anesthetic complications or presence of other co-morbidities, were excluded from this study. So this study was effectively carried out on 300 patients, of

Table 2 Criteria for easy or difficult laparoscopic cholecystectomy.

Easy	Difficult
• Time taken <60 min	• Time taken >60 min
• Absence of biliary leakage	• Presence of biliary leakage
• No injury to duct or artery	• Injury to duct or artery
• No conversion to open cholecystectomy	• Conversion to open cholecystectomy

talization, earlier return to normal activity, and better

Table 3 Performance of ultrasound scoring system with laparoscopic cholecystectomy as the reference standard.

		Laparoscopic cholecystectomy	
		Difficult	Easy
Ultrasound	Score >5	66	18
	Score ≤5	17	199

Table 4 Analysis of peroperative outcome with ultrasound parameters for statistical significance.

Ultrasound parameters		Difficult LC	Easy LC	p Value
Thickened GB wall	+	14	8	<0.05
	−	69	209	
Distended GB	+	21	15	<0.05
	−	62	202	
Impacted stones	+	5	3	<0.05
	−	78	214	
Dilated CBD	+	35	46	<0.05
	−	48	171	
Pericholecystic collection	+	1	5	~0.54
	−	82	212	
Multiple stones	+	27	65	~0.74
	−	56	152	
Enlarged liver	+	18	51	~0.67
	−	65	166	

Table 1 Ultrasound scoring system.

Ultrasound parameters	Score
GB wall thickness ≥4 mm	2
Transverse diameter of GB ≥5 cm	2
Presence of impacted stones	2
CBD diameter >6 mm	2
Presence of pericholecystic collection	1
Number of stones >1	1
Liver size ≥15.5 cm	1

predict easy (score of 5 or less) and difficult LC (score more than 5).

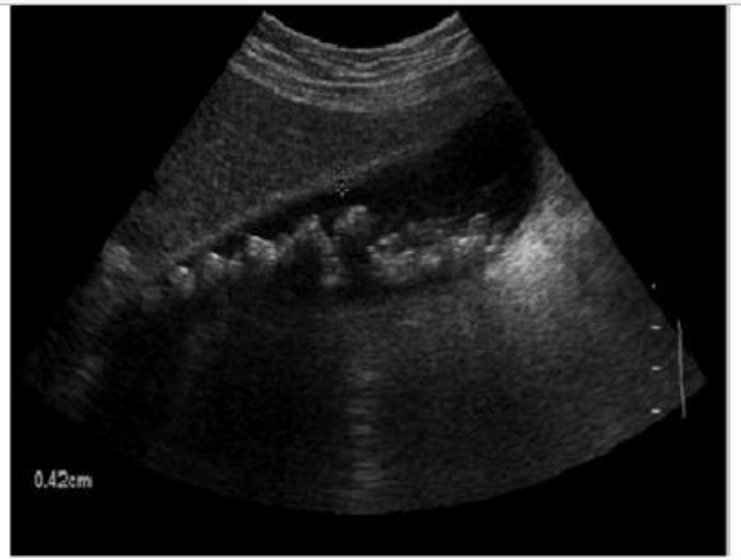

Figure 1 Longitudinal section of gallbladder region reveals multiple stones within gallbladder lumen with thickened (4.2 mm) gallbladder wall.

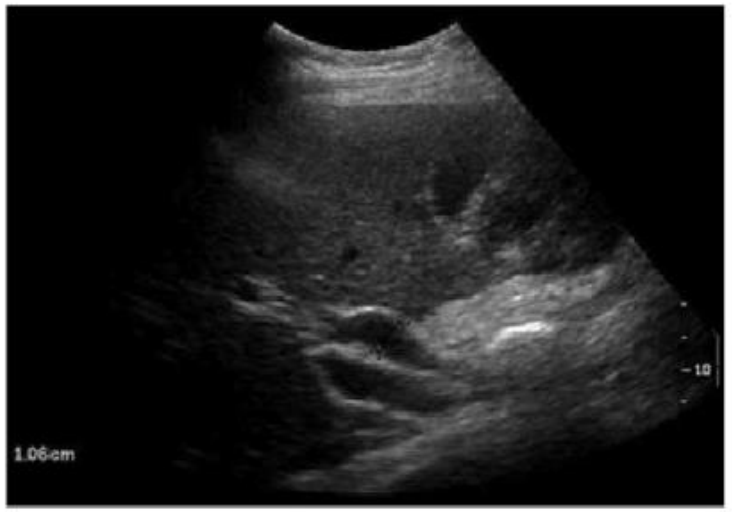

Figure 2 Longitudinal section of common bile duct reveals presence of a dilated duct (10.6 mm).

Use of Ultrasonography in Clarifying the Etiology of Anal Pain

Ashraf Talaat Youssef*

Department of Radiology, Faculty of Medicine, Fayoum University, Fayoum, Egypt

Received 14 February 2016; accepted 13 March 2017
Available online 3 May 2017

KEYWORDS
anal pain,
anorectal tumors,
perianal mass,
perianal sepsis,
three-dimensional ultrasound

Abstract *Introduction:* Anal pain is defined as pain originating from the anal canal or the perianal area that can be attributed to a variety of medical problems. The current study's aim was to evaluate the role of combined endoanal, transperineal, and in married women, transvaginal ultrasound in clarifying the etiology of anal pain among our patient study group.
Methodology: A total of 180 patients presented to our radiology department complaining of anal pain and were examined using transperineal, endoanal, and in women, transvaginal ultrasound aided with three-dimensional capability. The final diagnosis was reached, according to the surgical results and the histopathology reports in cases diagnosed with anorectal neoplasms and perianal masses.
Results: A total of 100 patients were diagnosed with perianal fistulas. Twenty-five cases presented with anal abscesses. In four cases, pilonidal sinus extended to the perianal spaces. Three cases had hiradenitis suppurativa, 13 cases showed occult anal sphincter defects, two cases had anorectal neoplasms, and one case was diagnosed with soft tissue ependymoma overlying the coccyx. Three cases were diagnosed with perianal soft tissue masses. One case was detected with recto vaginal fistulas, 10 cases showed thick internal anal sphincter, two cases had perianal cysts, and one case had perianal hematoma. Two cases showed hemorrhage in Douglas' pouch, and one case had pelvic collection sequelae of perforated pelvic appendicitis. Three cases had pelvic endometriosis; one case was detected with missed contraceptive device in the rectum. Three cases were diagnosed with prostatitis and two cases with prostatic abscesses. Two cases had prostatic carcinoma and one case had prostatic sarcoma.
Conclusion: The combined approaches of endoanal, transperineal, and in women, transvaginal ultrasound aided with three-dimensional capability proved highly valuable in clarifying the etiology of anal pain in our study group.

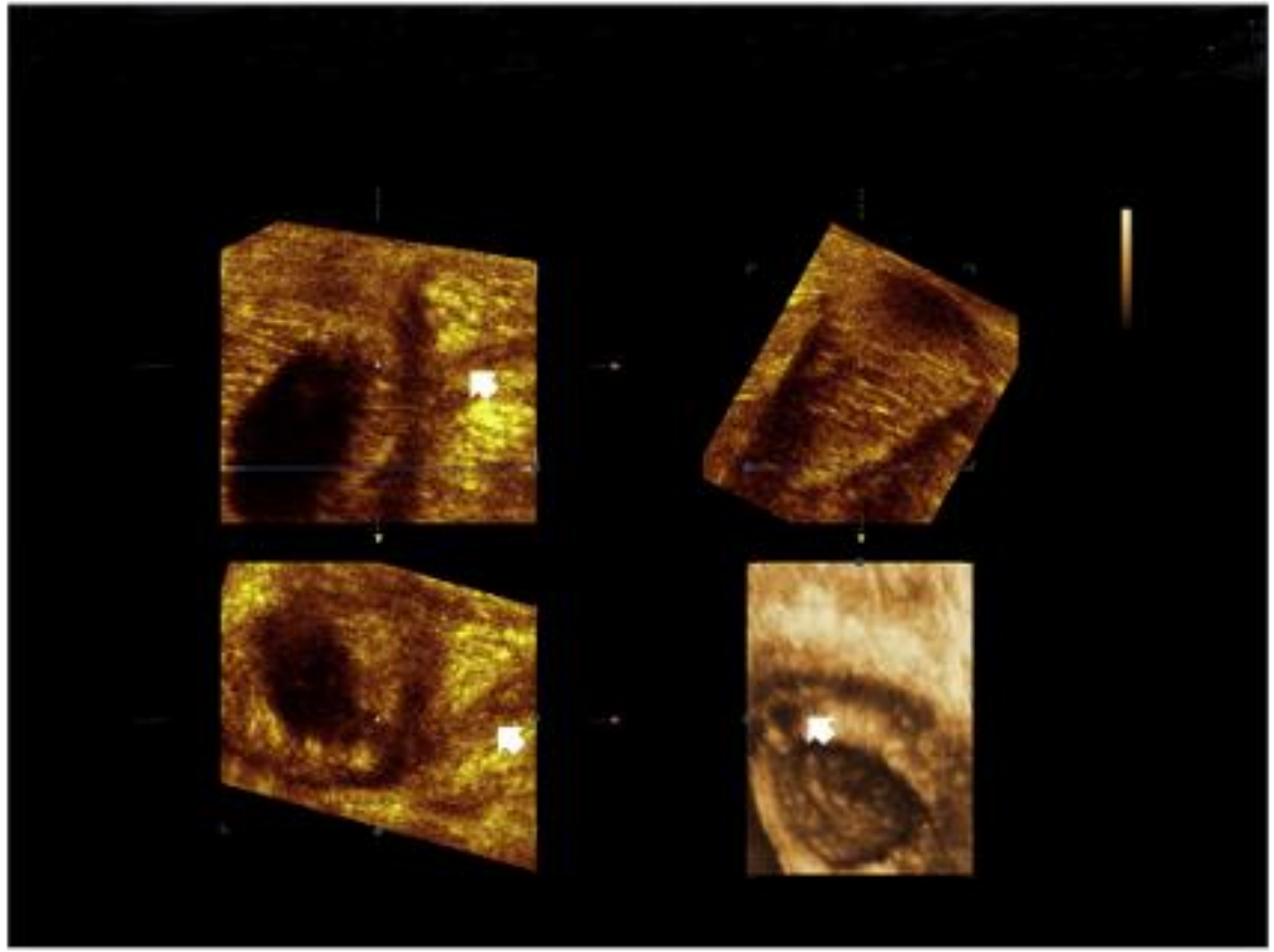

Figure 1 Three-dimensional reconstruction with multiplanar image analysis and volume rendering of trans-sphincteric perianal fistula (arrows).

Table 1 Demonstrating the number (%) and the sex of patients complaining of anal pain and their diagnosis.

Diagnosis	%	Sex		No. of cases
		Female	Male	
Perianal fistula	55.6	27	73	100
Anal abscess	13.9	10	15	25
Pilonidal sinus	2.2	—	4	4
Hiradenitis suppurativa	1.7	1	2	3
Thick internal sphincter	5.5	7	3	10
Occult sphincter tear	7.2	10	3	13
Anal tumor	0.55	—	1	1
Rectal tumor	0.55	1	—	1
Soft tissue ependymoma	0.55	1	—	1
Perianal masses	1.7	2	1	3
Hemorrhage in Douglas' pouch	1.1	2	—	2
Pelvic collection	0.55	1	—	1
Pelvic endometriosis	1.7	3	—	3
Missed loop in the rectum	0.55	1	—	1
Rectovaginal fistula	0.55	1	—	1
Prostatitis and prostatic abscess	2.8	—	5	5
Prostatic neoplasm	1.7	—	3	3
Perianal hematoma	0.55	1	—	1
Perianal cyst	1.1	2	—	2
	100	70	110	180

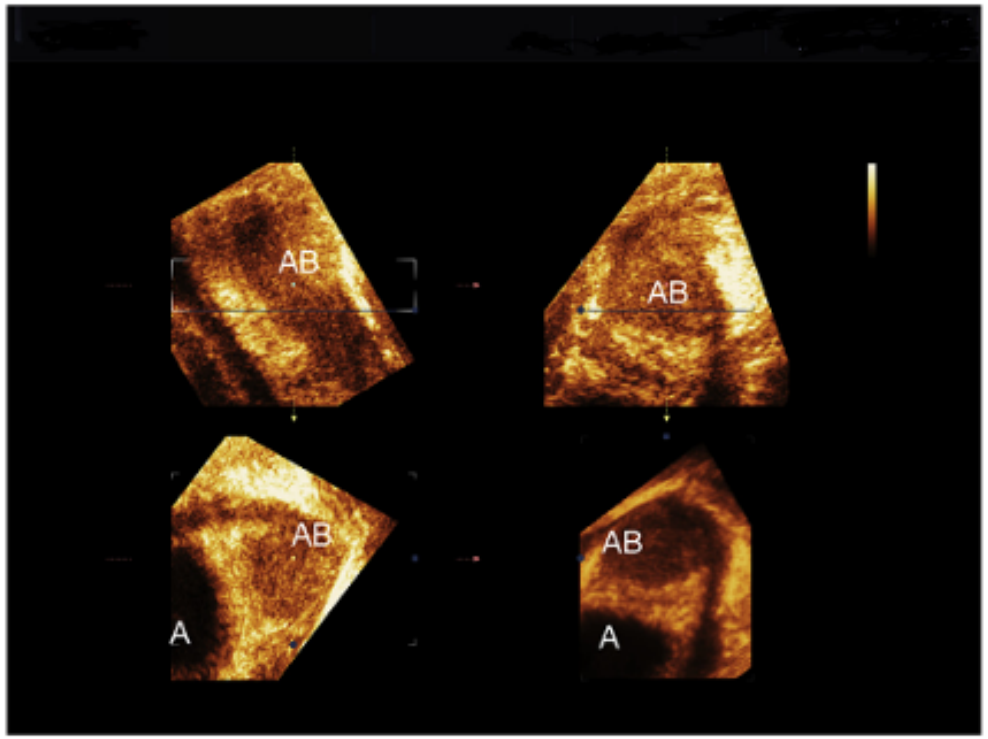

Figure 2 Three-dimensional reconstruction with multiplanar image analysis and volume rendering of ischiorectal abscess (AB).

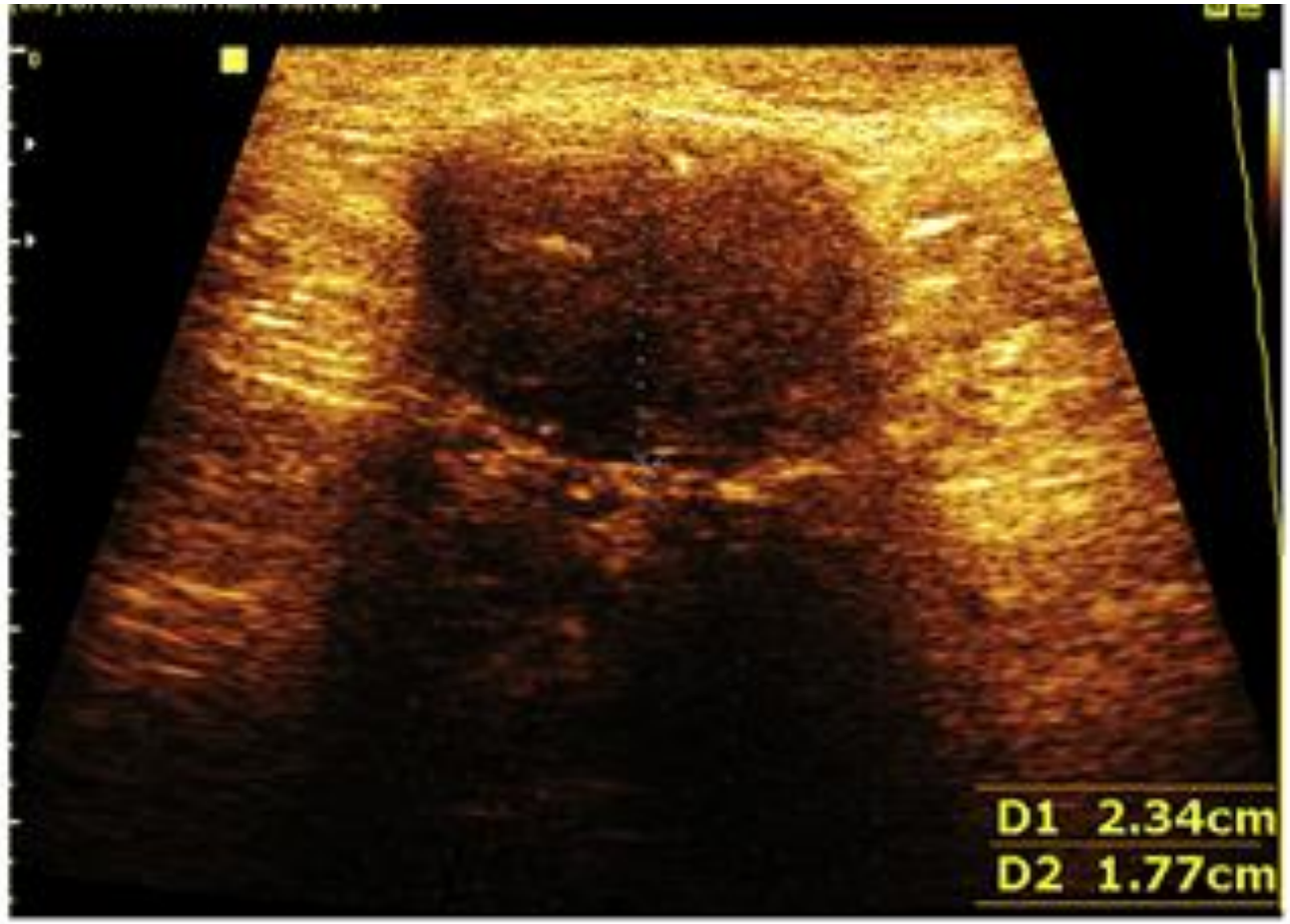

Figure 5 Two-dimensional ultrasound image of a well defined subcutaneous soft tissue mass overlying the coccyx (biopsy proven ependymoma).

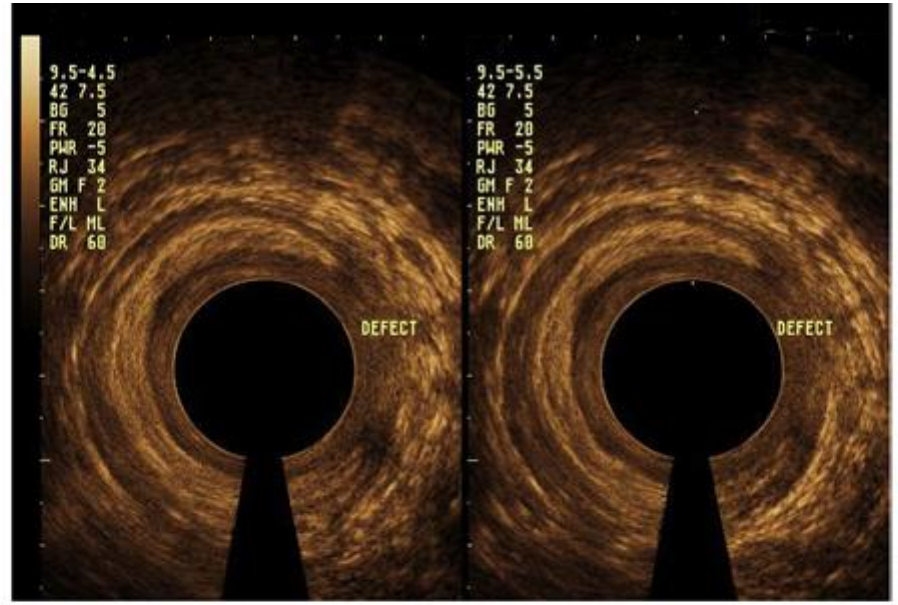

Figure 3 Two-dimensional endoanal ultrasound image of occult external anal sphincter defect.

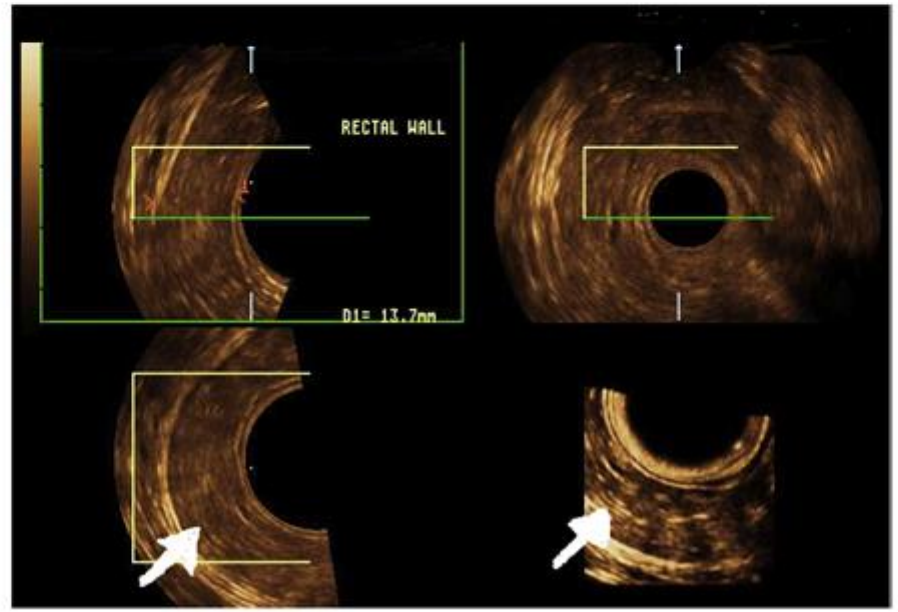

Figure 4 Three-dimensional endoanal ultrasound with multiplanar image analysis and volume rendering of circumferential infiltrative rectal neoplasm (arrows).

Effect of breath control on hepatic shear wave elasticity and dispersion in pediatric patients

Chanyoung Rhee[1], Seunghyun Lee[1], Young Hun Choi[1], Jae-Yeon Hwang[1], Jung-Eun Cheon[1,2]

[1]Department of Radiology, Seoul National University Hospital, Seoul National University College of Medicine, Seoul; [2]Institute of Radiation Medicine, Seoul National University Medical Research Center, Seoul, Korea

ULTRA SONO GRAPHY

ORIGINAL ARTICLE

https://doi.org/10.14366/usg.25037
eISSN: 2288-5943
Ultrasonography 2025;44:380-388

Purpose: This study aimed to evaluate the effect of breath control on the reliability of two-dimensional shear wave elastography (2D-SWE) and shear wave dispersion (SWD) measurements in pediatric patients.

Methods: This study included a retrospective cohort of 163 children and a prospective cohort of 27 children (aged 8–17 years). All participants underwent 2D-SWE and SWD under both free-breathing and breath-hold conditions between September 2021 and February 2023. The prospective cohort also underwent magnetic resonance elastography (MRE). Liver stiffness and dispersion values were compared between respiratory conditions. Inter- and intra-rater agreements were assessed, and correlations with MRE were analyzed in the prospective cohort.

Results: Liver stiffness and dispersion values were significantly higher during free-breathing compared to breath-hold (mean differences: 0.22 kPa and 0.39 m/s/kHz, respectively; both $P<0.01$). Breath-hold improved inter-rater agreement for 2D-SWE (intraclass correlation coefficient [ICC], 0.94 vs. 0.83; $P=0.005$) and SWD (ICC, 0.85 vs. 0.70; $P=0.048$). Intra-rater agreement for 2D-SWE (ICC, 0.88 vs. 0.88; $P>0.99$) and SWD (ICC, 0.70 vs. 0.74; $P=0.396$) remained moderate to good and did not differ significantly between conditions. The correlation between 2D-SWE and MRE was stronger under breath-hold than free-breathing ($r=0.73$ vs. $r=0.56$), although this difference was not statistically significant ($P=0.299$).

Conclusion: Breath-holding increases the reliability of pediatric 2D-SWE and SWD by improving inter-rater agreement and correlation with MRE. However, free-breathing also demonstrates comparable reproducibility with minimal bias, supporting its clinical feasibility for use in uncooperative pediatric patients.

Chinese Taipei Society of Ultrasound in Medicine

Available online at www.sciencedirect.com

ScienceDirect

journal homepage: www.jmu-online.com

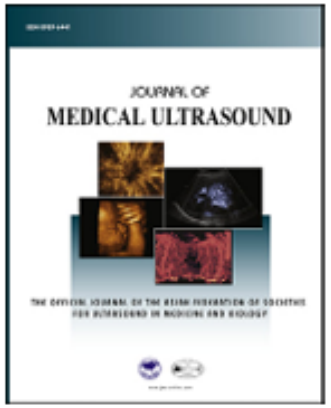

EDUCATIONAL FORUM

New Advances in Emergency Ultrasound Protocols for Shock

CME Credits

CrossMark

Jen-Tang Sun

Emergency Department, Far Eastern Memorial Hospital, Taiwan

Heart

Obstructive shock

Pericardial effusion with cardiac tamponad

Pulmonary embolism

Cardiogenic shock

Hypovolemic shock

Blood vessels

Inferior vena cava (IVC)

Hypovolemic shock

Obstructive shock/cardiogenic shock

Aorta

Femoral vein and popliteal vein

Abdomen

Hypovolemic shock

Septic shock

Lung

Obstructive shock

Hypovolemic shock

Cardiogenic shock

Figure 1 Pericardial effusion.

From Practical guide to Emergency ultrasound, chapter 5

Figure 2 RA collapse sign.

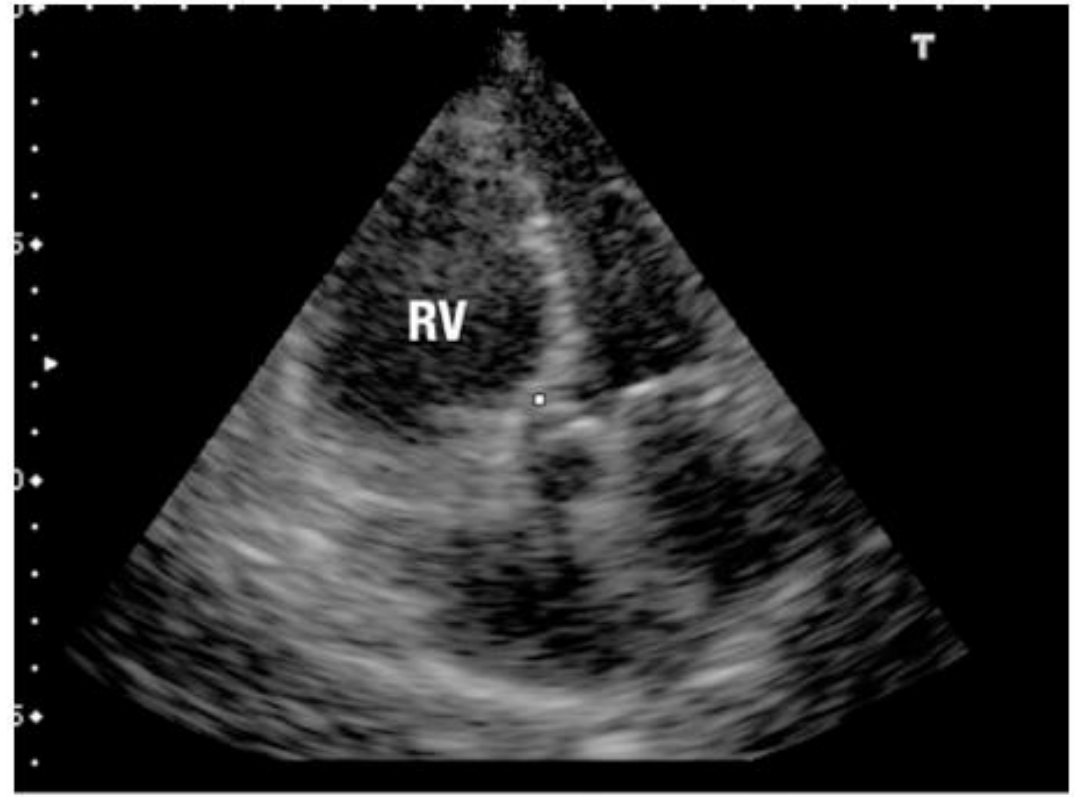

DISTENDED RV IN APICAL 4 CHAMBER VIEW

Figure 3 Pulmonary embolism.

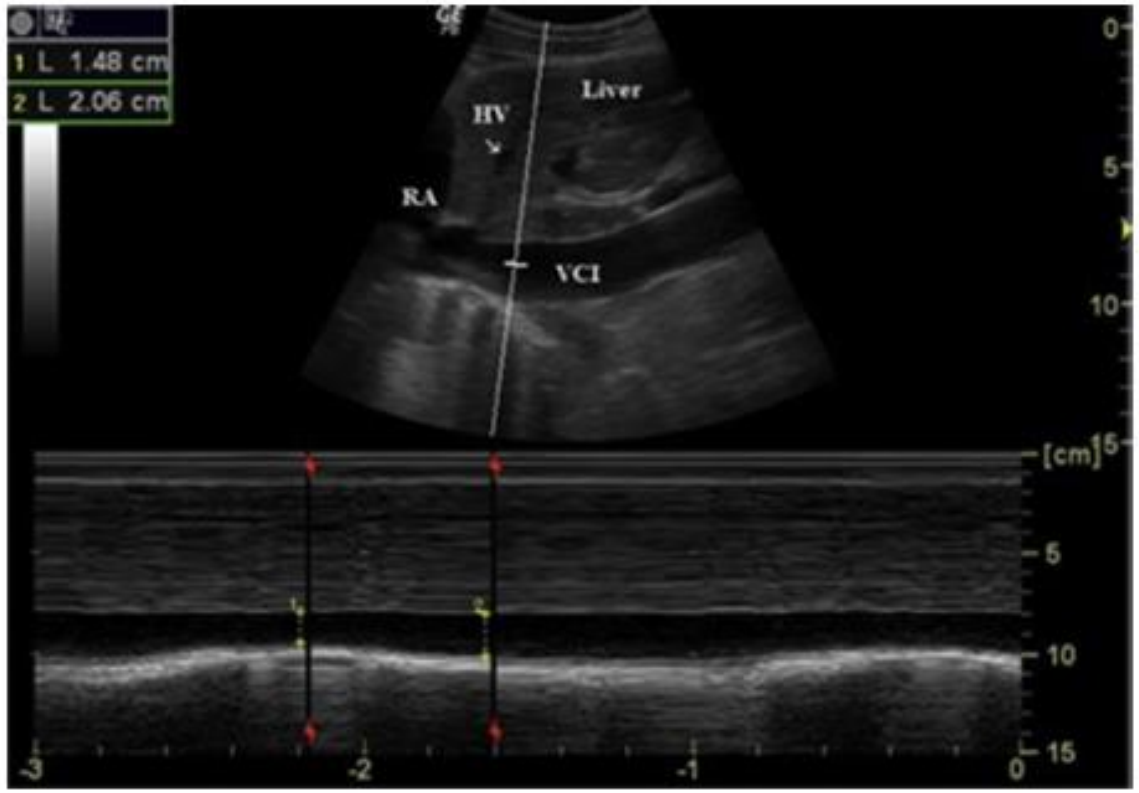

Figure 5 Size of IVCe and IVCi (from AJEM 2013; 31:763–767).

Figure 7 Intima flap over abdominal aorta.

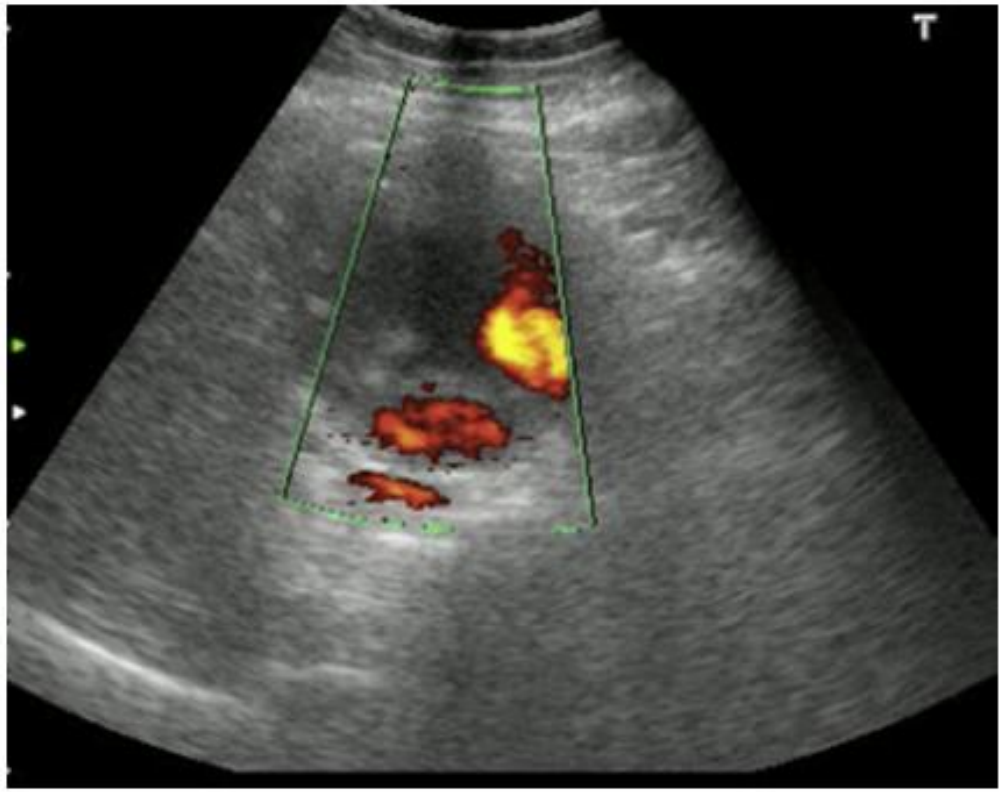

Figure 6 AAA > 5 cm.

Look for common sites of infection, for example, liver abscess and cholecystitis.

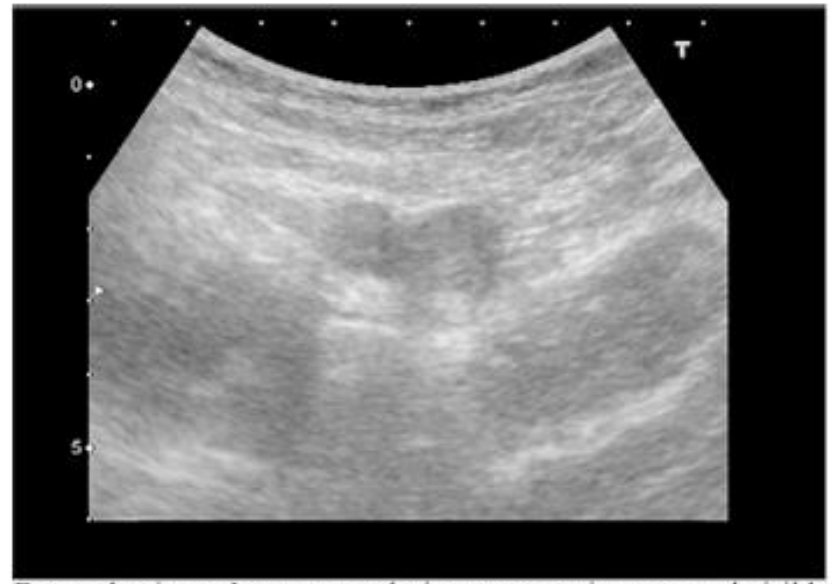

Femoral vein can't compress during compression test, and visible echogenic thrombosis inside vein

Figure 8 Deep vein thrombosis.

Echogenic free fluid over Doglus pouch

Figure 9 Hemoperitoneum in Doglus pouch.

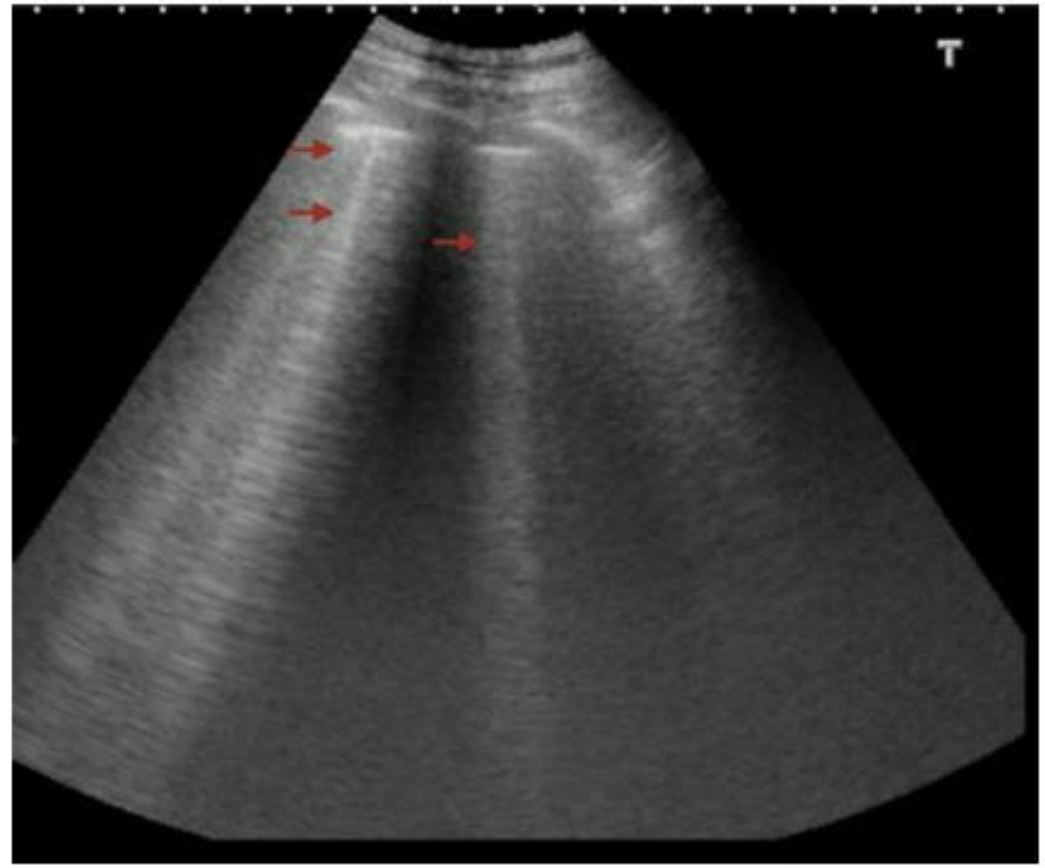

Figure 11 Multiple B line (arrow) in cardiogenic shock.

Measuring diaphragmatic excursion using 4-dimensional ultrasound: a feasibility study

ULTRA SONO GRAPHY

Adam Handley[1], Stephen Preece[1], Phil Tresadern[2], Katy Szczepura[1]

[1]School of Health and Society, University of Salford, Salford; [2]Visionomy, Salford, UK

TECHNICAL NOTE

https://doi.org/10.14366/usg.25020
eISSN: 2288-5943
Ultrasonography 2025;44:400-407

Four-dimensional ultrasound (4DUS) could provide more accurate characterisation of diaphragm function than existing M-mode ultrasound approaches. Therefore, the aim of this study was to investigate the feasibility of a novel method for tracking diaphragm excursion from 4DUS data. 4DUS was acquired from 12 participants who exhibited a range of breathing patterns. A custom algorithm tracked, reconstructed, and parameterized diaphragm movement using a sphere of time-varying radius. To validate the algorithm, a randomly selected slice of the sphere was sampled and compared to visual analysis. Agreement between the visual analysis and the algorithm was characterised using a Bland-Altman analysis. A root mean squared error (RMSE) metric was also calculated to quantify the fit between the ultrasound data and the spherical parametrisation. There was good agreement between the automated algorithm and visual analysis (bias, 0.09 cm; 95% limits of agreement, −0.44 to 0.25 cm). The RMSE metric was low (0.9–1.5 mm) across the 12 participants, demonstrating that the sphere was a good fit to the measured 4DUS data. This study demonstrates the feasibility of automated tracking of diaphragmatic excursion from 4DUS data using a sphere of time-varying radius. This technique may prove useful for diagnosing and monitoring breathing dysfunction.

Keywords: Diaphragm; Ultrasonography; Automated tracking; Four-dimensional ultrasound

Key points: Four-dimensional ultrasound (4DUS) allows the assessment of surface changes of an organ over time but to do this requires automation. We describe an algorithm that can automatically track diaphragm motion on 4DUS and reconstruct the imaged surface. This novel 4DUS technique is a first step towards changing how the diaphragm is imaged.

Received: February 1, 2025
Revised: June 23, 2025
Accepted: June 25, 2025

Correspondence to:
Adam Handley, MSc, School of Health and Society, University of Salford, Brian Blatchford Building, Manchester, M6 6PU, UK

Tel. +44-161-295-6758
E-mail: AMHandley-research@outlook.com

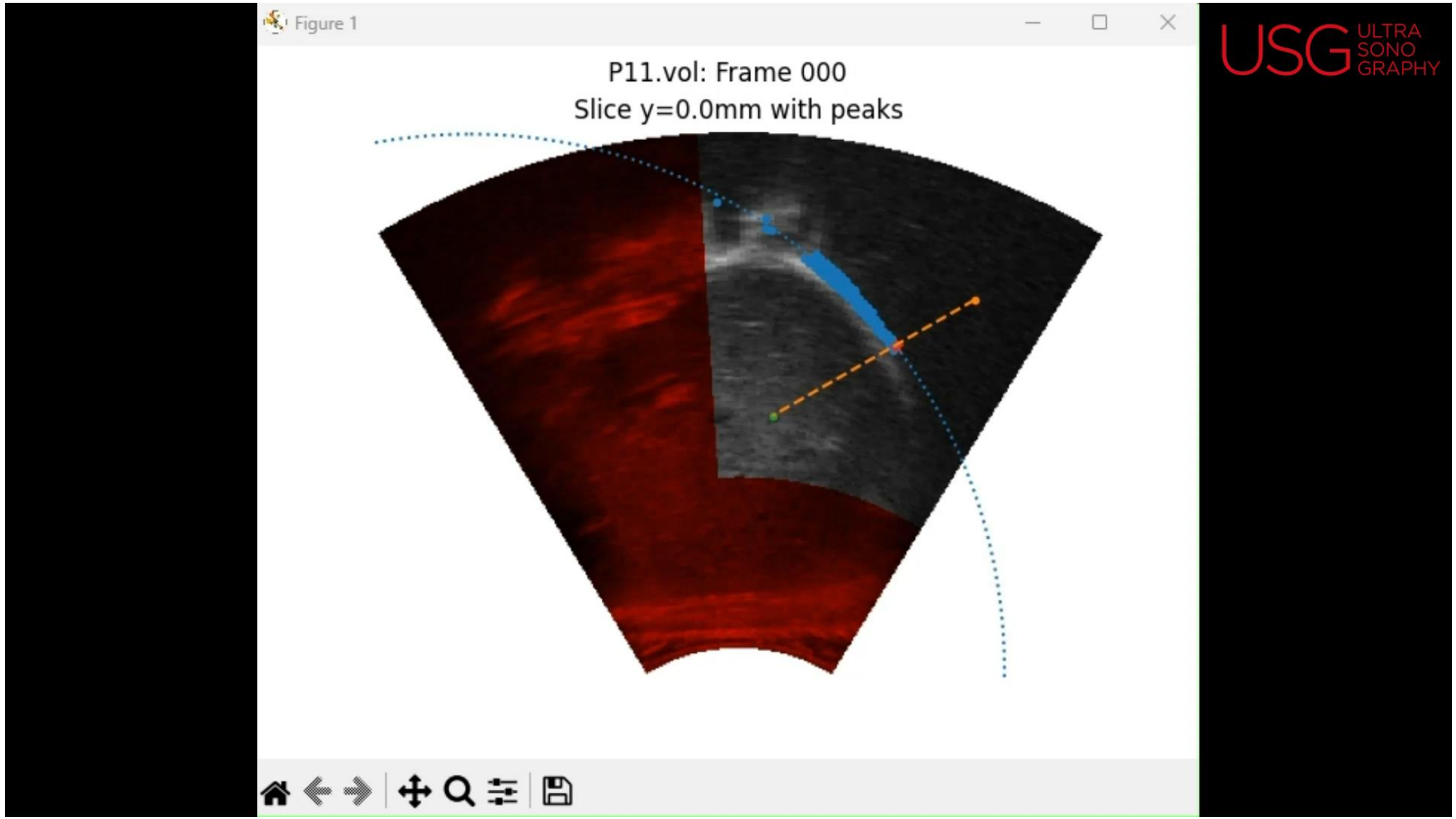
Figure 1
P11.vol: Frame 000
Slice y=0.0mm with peaks
USG
ULTRA
SONO
GRAPHY

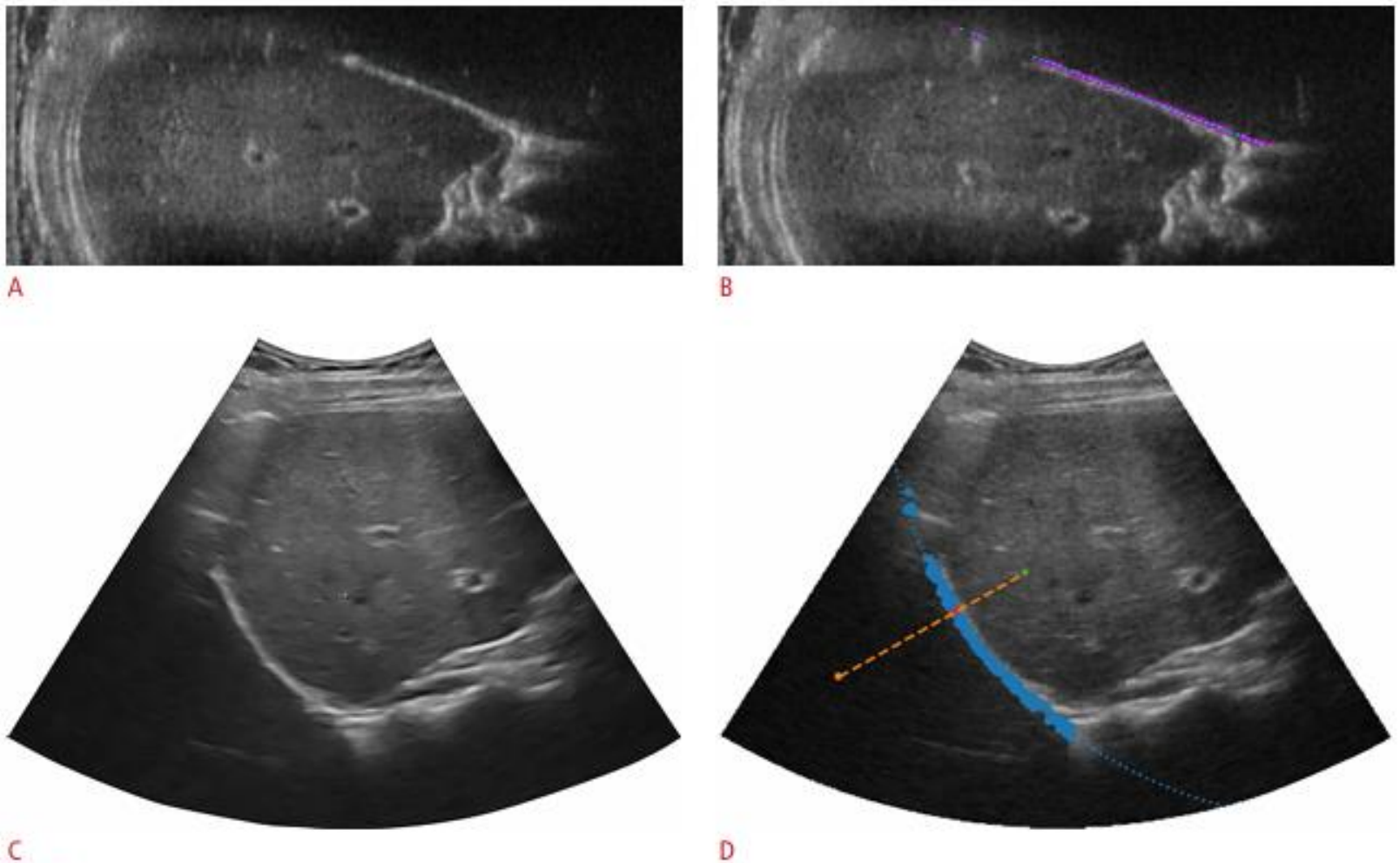

Fig. 2. **The diaphragm in the probe and Cartesian space.**
The diaphragm is shown as it appears in probe space (A) and Cartesian space (C). The algorithm identified points of interest of the diaphragm and fitted a plane (B) that is translated into an arc in Cartesian space (D). D also shows a motion line intersecting the arc which was used to quantify movement of the diaphragm.

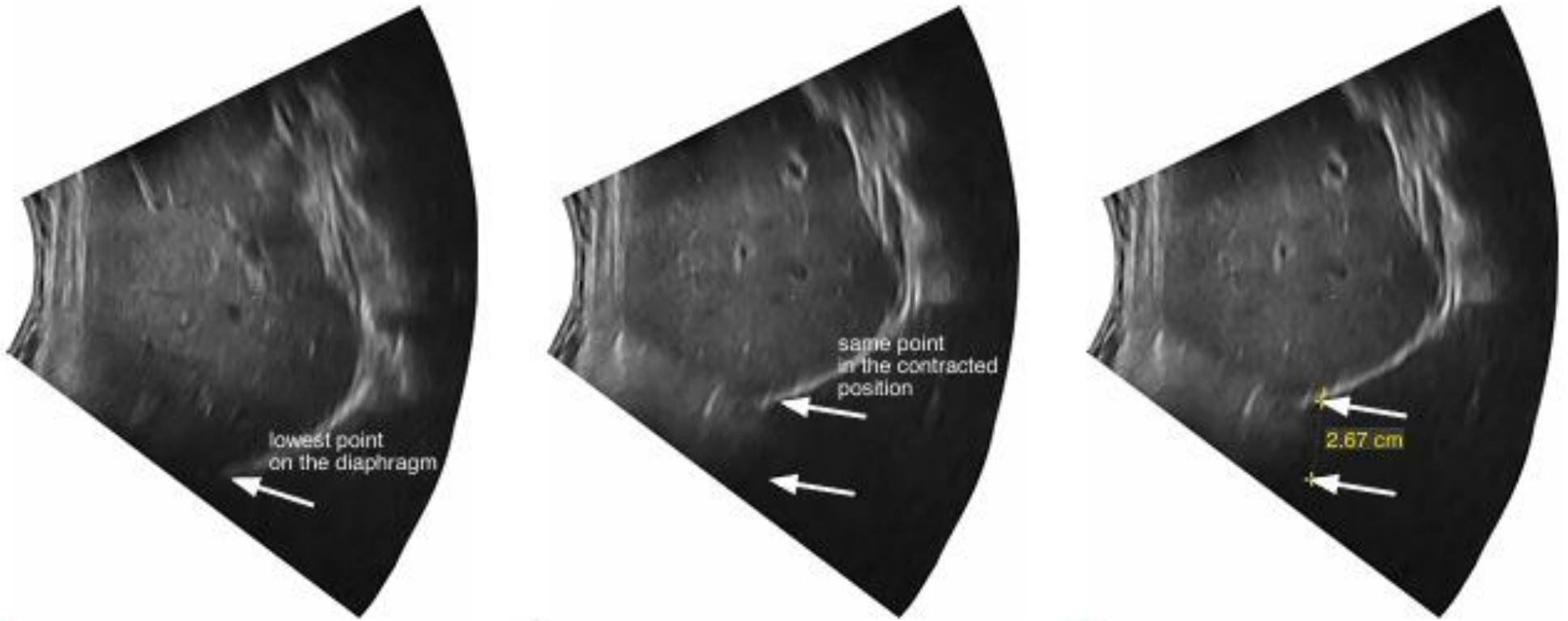

A B C

Fig. 3. Measurement of diaphragm excursion.
Rotated ultrasound images of the diaphragm in its relaxed positions (A) and its contracted position (B) so that the motion of the diaphragm is vertical. A and B show an annotation indicating the superior aspect of the diaphragm in each position. The distance between the two annotations is measured (C).